

Probing the decay mechanism of hot nuclei by Coulomb chronometry

D. GRUYER, E. BONNET, A. CHBIHI and J. D. FRANKLAND
for the INDRA COLLABORATION

GANIL, CEA-DSM/CNRS-IN2P3, Caen, France

Abstract

In this contribution, we propose a new Coulomb chronometer suitable for three-fragment exit channels. We use this chronometer to extract the evolution of the fragment emission time in $^{129}\text{Xe}+^{cat}\text{Sn}$ central collisions from 12 to 25 MeV/A bombarding energy. The involved time scale becomes compatible with simultaneous three-fragment break-up above $E^* = 4.0 \pm 0.5$ MeV/A, which can be interpreted as the energy required for the onset of multifragmentation.

1 Introduction

Recent data on $^{129}\text{Xe}+^{cat}\text{Sn}$ central collisions [1] show that at 8 MeV/A bombarding energy, almost all the reaction cross section is composed of events with two heavy fragments in the exit channel (see Fig. 1(a)). Above 12 MeV/A bombarding energy, the three-fragment exit channel becomes significant, overcoming the two-fragment production rate above 18 MeV/A. The decay mechanism responsible for these three-fragment events is not well established: Is it the continuation of low energy fission or the precursor of high energy simultaneous fragmentation? To answer this question, a dynamical characterization of the decay mechanism is needed. In particular, the estimation of the involved time scales may allow to disentangle sequences of two binary fission from simultaneous three-fragment break-up.

In this contribution, we propose a new Coulomb chronometer suitable for three-fragment exit channels. We use this chronometer to extract the evolution of the fragment emission time in $^{129}\text{Xe}+^{cat}\text{Sn}$ central collisions from 12 to 25 MeV/A bombarding energy.

2 Experimental analysis

Collisions of $^{129}\text{Xe} + {}^{cat}\text{Sn}$ at 12, 15, 18, 20, and 25 MeV/A were measured using the INDRA 4π charged product array [2] at the GANIL accelerator facility. In this analysis, we considered only fusion-like events leading to three heavy fragments ($Z > 10$) in the exit channel. Fusion-like events were selected by requiring at least 90% of the total charge of the system to be detected.

We start from the hypothesis that fragments are produced sequentially. If two successive splittings occur, three possible sequences of splittings have to be considered.

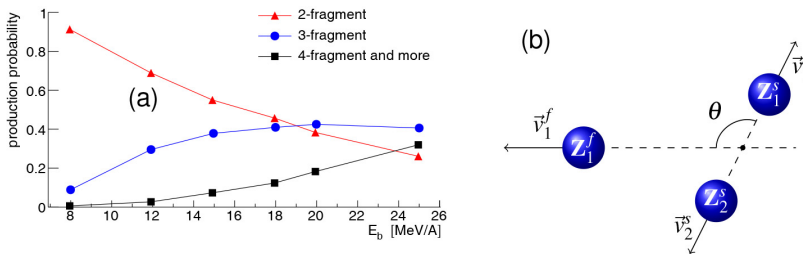


Figure 1: (color online). (a) Evolution of different exit channel probabilities as a function of the beam energy for $^{129}\text{Xe} + {}^{cat}\text{Sn}$ central collisions. (b) Definition of the relevant kinematic observables for the three-fragment exit channel, in the rest frame of the intermediate system Z_2^f .

To identify the sequence of splittings event by event, we compare the relative velocity between each pair of fragments with that expected for fission, taken from the Viola systematics [3, 4]. The pair with the most Viola-like relative velocity is considered to have been produced during the second splitting. We can therefore trivially deduce that the remaining fragment was emitted first. Once the sequence of splittings is known event by event, fragments can be sorted according to their order of production. Let us now call Z_1^f and Z_2^f , the two nuclei coming from the first splitting. The fragment Z_2^f breaks in Z_1^s and Z_2^s during the second step (see Fig. 1).

To estimate the mean inter-splitting time, we used the correlation between the inter-splitting angle θ and the relative velocity of the second splitting: $v_{12}^s = \|\vec{v}_1^s - \vec{v}_2^s\|$ (see Fig. 2(a)). These correlations present a maximum at $\theta \sim 90$, which is more pronounced as the beam energy increases. We quantify this effect by the Coulomb distortion parameter $\delta v = v_{12}^s(90) - v_{12}^s(0)$ which increases with increasing beam energy (Fig. 2(b)), indicating that the second splitting occurred closer and closer to the first emitted fragment. To

translate δv in terms of inter-splitting time δt , we performed Coulomb trajectory calculations for point charges, which simulate sequential break-ups using experimental mean charges. Finally, we obtained the evolution of the inter-splitting time as a function of the beam energy (Fig.3).

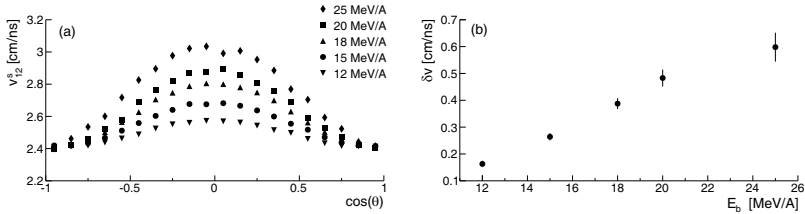


Figure 2: (a) Correlation between the inter-splitting angle θ and the relative velocity of the second splitting v_{12}^s , vertical error bars are smaller than the size of the points; (b) evolution of the Coulomb distortion parameter δv as a function of the beam energy for $^{129}\text{Xe}+^{cat}\text{Sn}$ central collisions.

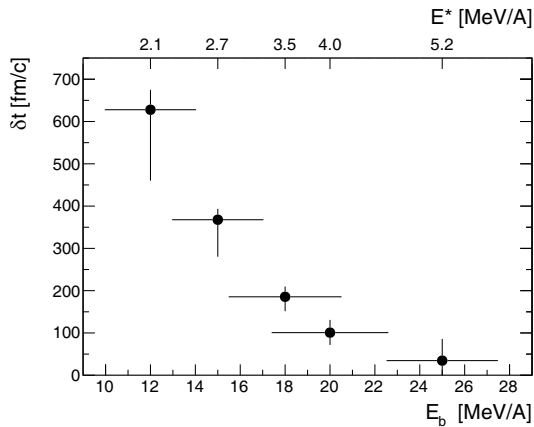


Figure 3: Evolution of the mean inter-splitting time δt as a function of the beam energy (lower scale) and the estimated excitation energy of the incomplete fusion source (upper scale) produced in $^{129}\text{Xe}+^{cat}\text{Sn}$ central collisions. Horizontal error bars refer to the upper scale.

3 Discussion

A clear decrease of the inter-splitting time with increasing beam energy is observed in Fig.3. At 12 MeV/A, the inter-splitting time δt is of the order of 600 fm/c. It shows that, for the lower beam energies, fragments arise from

two successive splittings, validating our starting hypothesis. As the beam energy increases from 12 MeV/A to 20 MeV/A, δt decreases monotonically from 600 fm/c to about 100 fm/c. Above 20 MeV/A, δt becomes compatible with zero. Our trajectory calculations show that, below $\delta t \sim 100$ fm/c, fragment emissions can not be treated independently, and it is no longer meaningful to speak of a sequential process. Therefore, Fig.3 shows that the three-fragment exit channel is compatible with successive binary splittings on shorter and shorter time scales, becoming indistinguishable from simultaneous three-fragment break-up at bombarding energies above 20 MeV/A, which correspond to $E^* \sim 4 \pm 0.5$ MeV/A.

4 Conclusion

In summary, we proposed a new chronometer which takes advantage of Coulomb proximity effects observed in the three-fragment final state. This is made possible thanks to the highly exclusive measurement performed with INDRA. We have shown that these fragments arise from successive binary splittings occurring on shorter and shorter time scales.

The involved time scale becomes compatible with simultaneous three-fragment break-up above $E^* = 4.0 \pm 0.5$ MeV/A, which can be interpreted as the signature of the onset of multifragmentation.

References

- [1] A. Chbihi, L. Manduci et al., *J. Phys.: Conf. Ser.* **420** 012099 (2013).
- [2] J. Pouthas, B. Borderie et al., *Nucl. Instrum. Methods Phys. Res., Sect A* **357** 418 (1995).
- [3] V.E. Viola, K. Kwiatkowski and M. Walker, *Phys. Rev. C: Nucl. Phys.*, **31** 1550 (1985).
- [4] D. Hinde, J. Leigh et al., *Nucl. Phys. A* **472** 318 (1987).